

Electronic supplementary material

Insight into the structure and redox chemistry of [carbonatotetraamminecobalt(III)] permanganate and its monohydrate as Co-Mn-oxide catalyst precursors of the Fischer-Tropsch synthesis

Kende Béres^{1,2}, Zsolt Dúrvanger^{3,4}, Zoltán Homonnay⁵, Laura Bereczki^{1,6}, Berta Barta Holló⁷, Attila Farkas⁸, Vladimir M.Petrusevski⁹ and László Kótai^{1,10*}

¹ Institute of Materials and Environmental Chemistry, HUN-REN Research Centre for Natural Sciences, Budapest, Hungary; beres.kende.attila@ttk.hu (K.A.B.); nagyne.bereczki.laura@ttk.mta.hu (L.B.)

² György Hevesy PhD School of Chemistry, ELTE Eötvös Loránd University, Budapest, Hungary

³ Structural Chemistry and Biology Laboratory, Institute of Chemistry, ELTE Eötvös Loránd University, Budapest, Hungary

⁴ ELKH-ELTE Protein Modelling Research Group, Budapest, Hungary; zsolt.durvanger@ttk.elte.hu

⁵ Institute of Chemistry, ELTE Eötvös Loránd University, Budapest, Hungary; homonnay.zoltan@ttk.elte.hu

⁶ Centre for Structural Science, HUN-REN Research Centre for Natural Sciences, H-1117 Budapest, Hungary

⁷ Department of Chemistry, Biochemistry and Environmental Protection, Faculty of Sciences, University of Novi Sad, Novi Sad, Serbia

⁸ Department of Organic Chemistry and Technology, Faculty of Chemical Technology and Biotechnology, Budapest University of Technology and Economics, Budapest, Hungary; farkas.attila@vbk.bme.hu

⁹ Faculty of Natural Sciences and Mathematics, Ss. Cyril and Methodius University, MK-1000 Skopje, North Macedonia; vladop@pmf.ukim.mk

¹⁰ Deuton-X Ltd., H-2030, Érd, Hungary

* Correspondence: kotai.laszlo@ttk.hu.

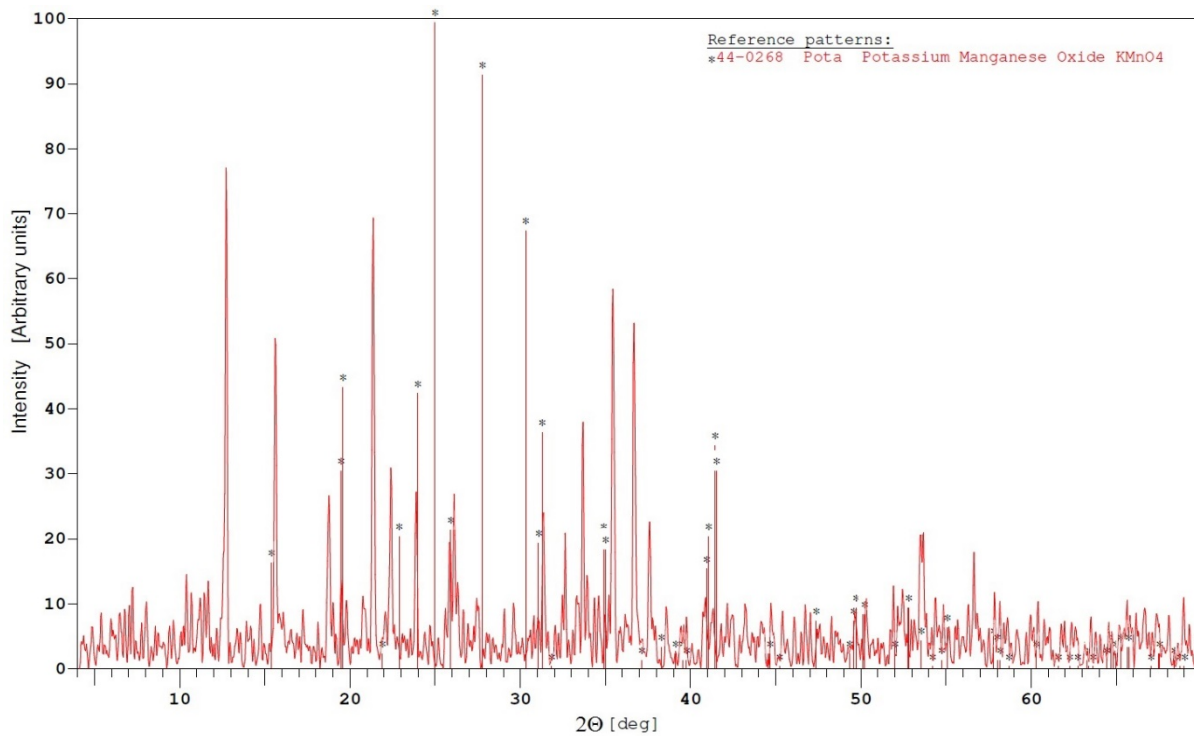


Figure S1 Powder-XRD study of the reaction product of synthesis root described in ref. [4].

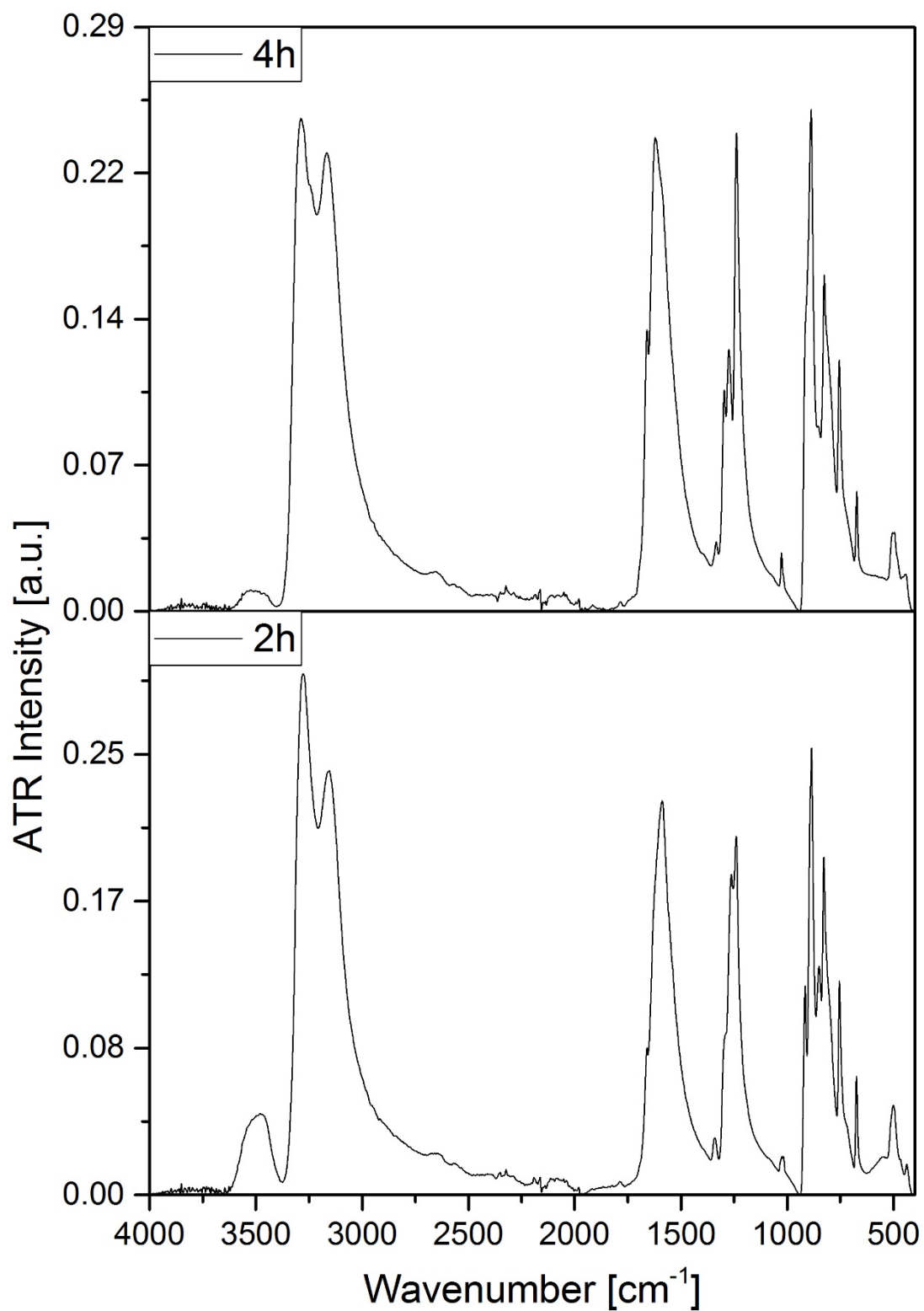


Figure S2 Analytical range IR study of heat treatment residues of compound **2**.

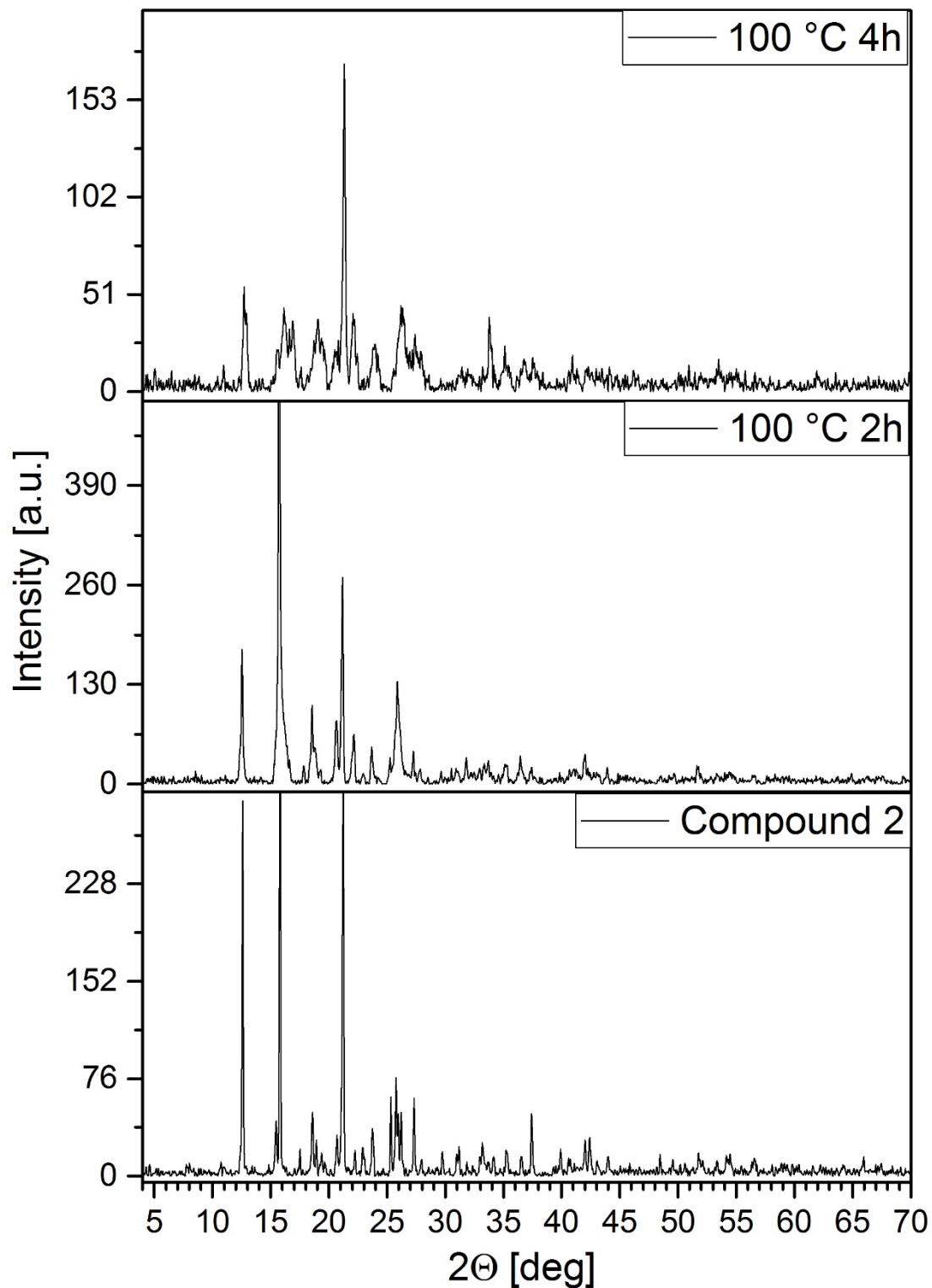


Figure S3 Powder-XRD of Compound 2, partially (2 h), and completely dehydrated products (4 h) – Compound 1.

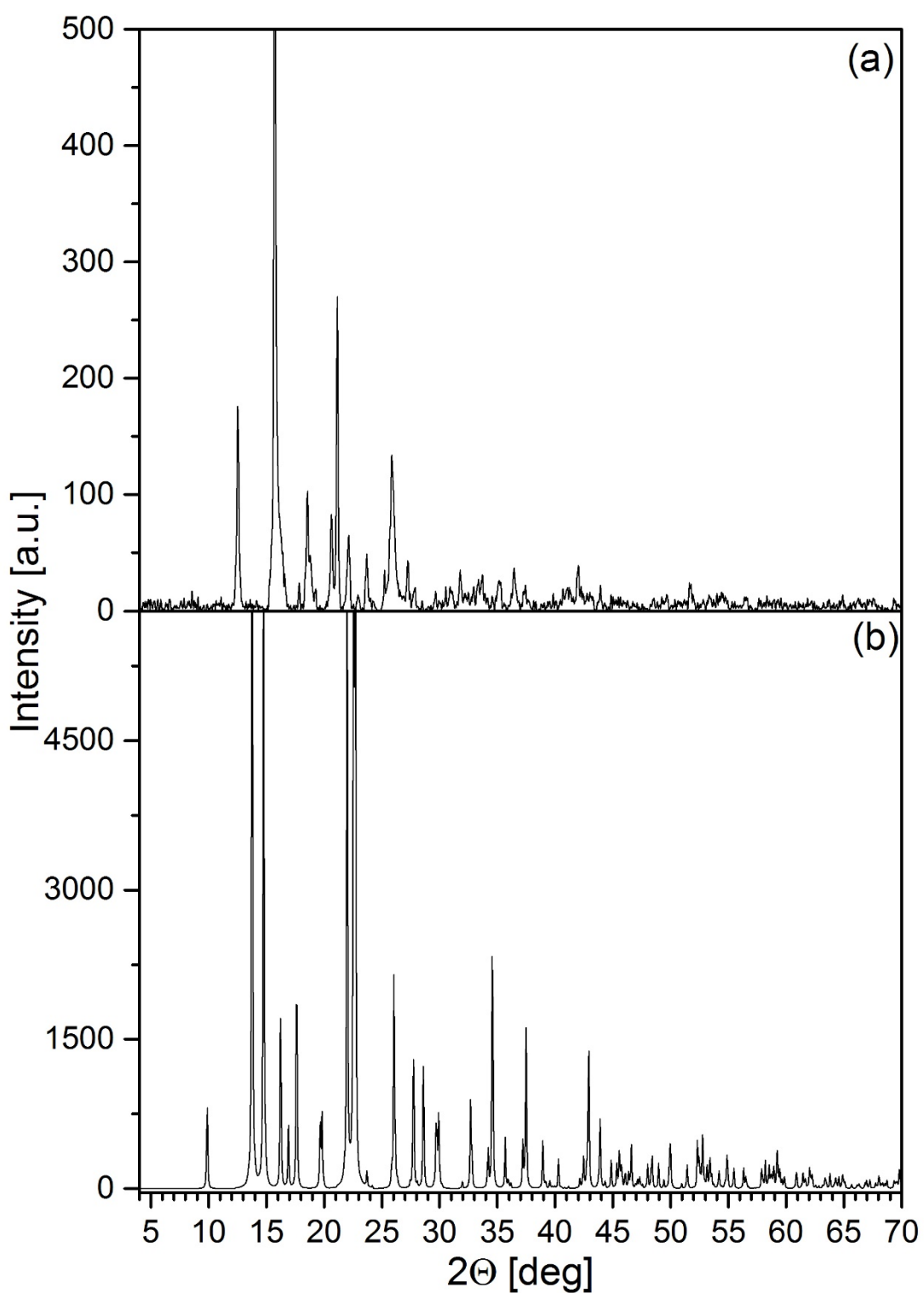


Figure S4 Powder-XRD of (a) Compound **1** and (b) $[\text{Co}(\text{NH}_3)_4\text{CO}_3]\text{ClO}_4$.

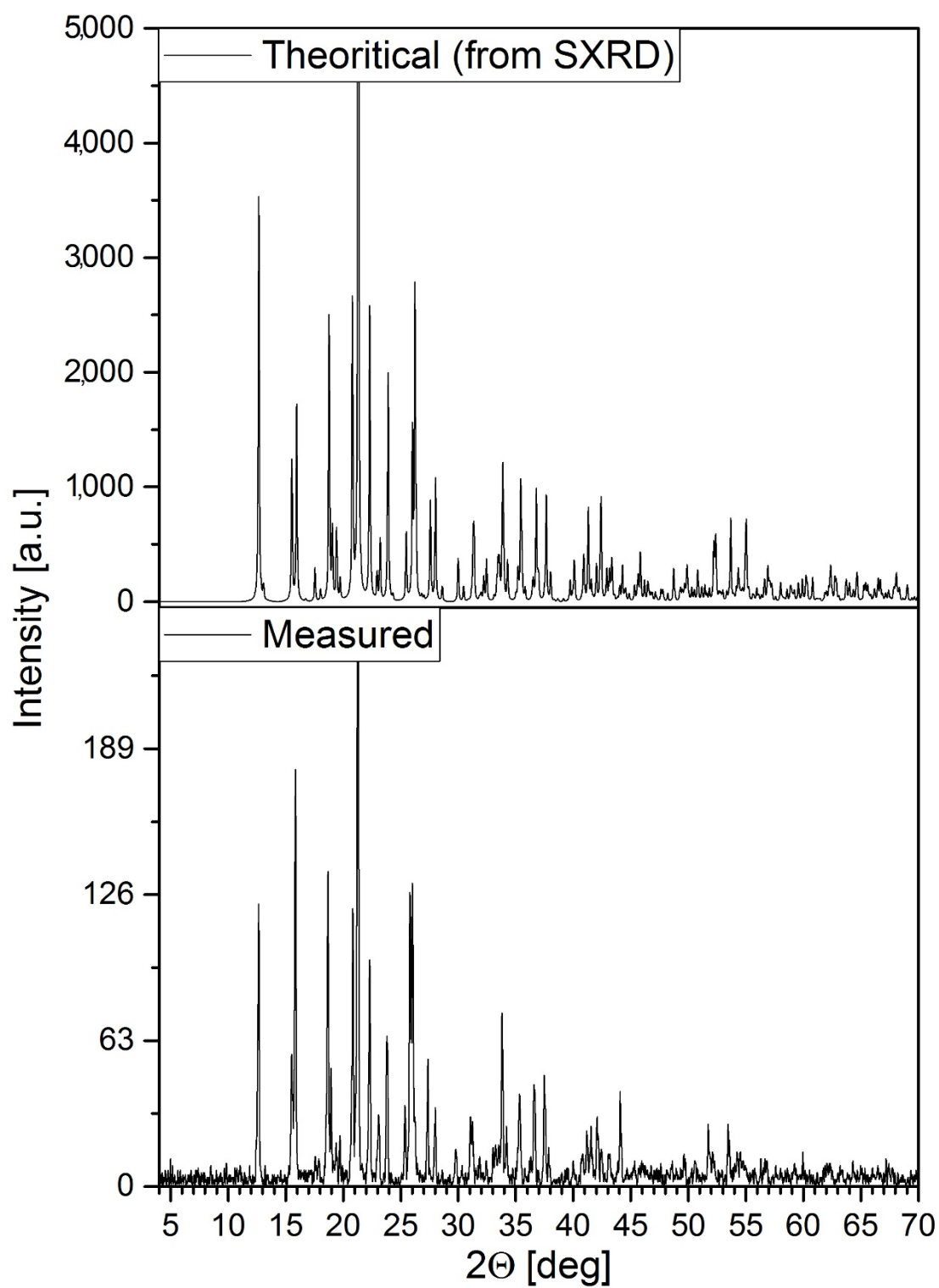


Figure S5 Measured and theoretical Powder-XRD of Compound 2.

Table S1 Crystallographic parameters of the orthorhombic compound **2**.

Empirical formula	C H14 Co Mn N4 O8	
Formula weight	324.03	
Temperature	101.1(6) K	
Wavelength	1.54184 Å	
Crystal system	Orthorhombic	
Space group	Pbca	
Unit cell dimensions	$a = 11.10180(10)$ Å	$\alpha = 90^\circ$.
	$b = 10.57700(10)$ Å	$\beta = 90^\circ$.
	$c = 17.06750(10)$ Å	$\gamma = 90^\circ$.
Volume	2004.13(3) Å ³	
Z	8	
Density (calculated)	2.148 Mg/m ³	
Absorption coefficient	23.593 mm ⁻¹	
F(000)	1312	
Crystal size	0.114 x 0.081 x 0.034 mm ³	
Theta range for data collection	5.183 to 75.421°.	
Index ranges	-13<=h<=13, -13<=k<=12, -21<=l<=21	
Reflections collected	58908	
Independent reflections	2073 [R(int) = 0.0429]	
Completeness to theta = 67.684°	100.0 %	
Absorption correction	Analytical	
Max. and min. transmission	0.572 and 0.208	
Refinement method	Full-matrix least-squares on F ²	
Data / restraints / parameters	2073 / 0 / 144	
Goodness-of-fit on F ²	1.126	
Final R indices [I>2sigma(I)]	R1 = 0.0224, wR2 = 0.0505	
R indices (all data)	R1 = 0.0228, wR2 = 0.0506	
Extinction coefficient	0.00014(3)	
Largest diff. peak and hole	0.307 and -0.267 e·Å ⁻³	

Table S2 Bond lengths [Å] and angles [°] in the structure of compound **2**.

Co(1)-O(2)	1.9252(14)
Co(1)-O(1)	1.9273(13)
Co(1)-N(1)	1.9389(16)
Co(1)-N(3)	1.9511(17)
Co(1)-N(2)	1.9538(16)
Co(1)-N(4)	1.9543(16)
Co(1)-C(1)	2.3303(19)
Mn(1)-O(5)	1.6103(14)
Mn(1)-O(6)	1.6183(15)
Mn(1)-O(7)	1.6210(14)
Mn(1)-O(4)	1.6249(15)
O(2)-C(1)	1.318(2)
O(1)-C(1)	1.310(2)
O(3)-C(1)	1.242(2)
O(2)-Co(1)-O(1)	68.62(6)
O(2)-Co(1)-N(1)	97.39(6)
O(1)-Co(1)-N(1)	165.97(6)
O(2)-Co(1)-N(3)	168.88(6)
O(1)-Co(1)-N(3)	100.32(6)
N(1)-Co(1)-N(3)	93.64(7)
O(2)-Co(1)-N(2)	91.00(6)
O(1)-Co(1)-N(2)	88.48(6)
N(1)-Co(1)-N(2)	90.87(7)
N(3)-Co(1)-N(2)	87.45(7)
O(2)-Co(1)-N(4)	89.75(6)
O(1)-Co(1)-N(4)	89.83(6)
N(1)-Co(1)-N(4)	91.13(7)
N(3)-Co(1)-N(4)	91.41(7)
N(2)-Co(1)-N(4)	177.76(7)
O(2)-Co(1)-C(1)	34.43(6)
O(1)-Co(1)-C(1)	34.20(6)
N(1)-Co(1)-C(1)	131.79(7)
N(3)-Co(1)-C(1)	134.48(7)
N(2)-Co(1)-C(1)	89.06(7)
N(4)-Co(1)-C(1)	90.37(7)

O(5)-Mn(1)-O(6)	110.17(8)
O(5)-Mn(1)-O(7)	109.00(7)
O(6)-Mn(1)-O(7)	108.84(8)
O(5)-Mn(1)-O(4)	109.89(8)
O(6)-Mn(1)-O(4)	109.32(7)
O(7)-Mn(1)-O(4)	109.60(8)
C(1)-O(2)-Co(1)	89.86(11)
C(1)-O(1)-Co(1)	90.01(11)
O(3)-C(1)-O(1)	124.56(17)
O(3)-C(1)-O(2)	123.95(17)
O(1)-C(1)-O(2)	111.48(16)
O(3)-C(1)-Co(1)	177.75(15)
O(1)-C(1)-Co(1)	55.80(9)
O(2)-C(1)-Co(1)	55.71(9)

Table S3 Atomic coordinates ($\times 10^4$) and equivalent isotropic displacement parameters ($\text{\AA}^2 \times 10^3$) in compound **2**. U(eq) is defined as one-third of the trace of the orthogonalized U^{ij} tensor.

	x	y	z	U(eq)
Co(1)	6421(1)	5173(1)	6144(1)	7(1)
Mn(1)	7719(1)	7630(1)	3399(1)	10(1)
O(2)	6822(1)	6942(1)	6094(1)	11(1)
O(1)	5234(1)	6110(1)	5559(1)	10(1)
O(3)	5581(1)	8196(1)	5388(1)	14(1)
O(7)	7861(1)	9151(1)	3323(1)	15(1)
O(4)	6472(1)	7185(1)	2984(1)	17(1)
O(6)	8845(1)	6960(1)	2963(1)	19(1)
O(5)	7704(1)	7251(1)	4312(1)	20(1)
O(8)	4950(1)	10558(2)	6042(1)	19(1)
N(1)	7812(1)	4627(2)	6742(1)	11(1)
N(4)	5511(2)	5480(2)	7106(1)	12(1)
N(3)	5762(2)	3469(2)	6057(1)	12(1)
N(2)	7270(2)	4854(2)	5162(1)	12(1)
C(1)	5855(2)	7149(2)	5665(1)	10(1)

Table S4 Anisotropic displacement parameters ($\text{\AA}^2 \times 10^3$ in compound **2**. The anisotropic displacement factor exponent takes the form: $-2\pi^2[h^2a^2U^{11} + \dots + 2hka \cdot b \cdot U^{12}]$.

	U ¹¹	U ²²	U ³³	U ²³	U ¹³	U ¹²
Co(1)	9(1)	6(1)	8(1)	0(1)	0(1)	0(1)
Mn(1)	13(1)	9(1)	10(1)	0(1)	1(1)	0(1)
O(2)	12(1)	8(1)	12(1)	0(1)	-1(1)	-1(1)
O(1)	12(1)	8(1)	11(1)	0(1)	-2(1)	0(1)
O(3)	16(1)	9(1)	15(1)	2(1)	0(1)	2(1)
O(7)	17(1)	13(1)	15(1)	2(1)	1(1)	0(1)
O(4)	15(1)	17(1)	18(1)	-3(1)	1(1)	-1(1)
O(6)	17(1)	18(1)	21(1)	-6(1)	3(1)	2(1)
O(5)	31(1)	14(1)	14(1)	2(1)	3(1)	-3(1)
O(8)	23(1)	15(1)	18(1)	-2(1)	-5(1)	5(1)
N(1)	12(1)	10(1)	10(1)	1(1)	-1(1)	1(1)
N(4)	12(1)	12(1)	12(1)	2(1)	1(1)	1(1)
N(3)	13(1)	11(1)	13(1)	1(1)	-1(1)	0(1)
N(2)	15(1)	9(1)	11(1)	1(1)	0(1)	1(1)
C(1)	11(1)	9(1)	9(1)	-2(1)	3(1)	1(1)

Table S5 Hydrogen coordinates ($\times 10^4$) and isotropic displacement parameters ($\text{\AA}^2 \times 10^3$) in compound **2**.

	x	y	z	U(eq)
H(8A)	4793	11067	5655	28
H(8B)	4865	9780	5887	28
H(1A)	8482	5027	6560	13
H(1B)	7905	3777	6689	13
H(1C)	7702	4822	7256	13
H(4A)	4713	5540	6991	14
H(4B)	5765	6215	7329	14
H(4C)	5632	4830	7446	14
H(3A)	5356	3393	5596	15
H(3B)	5250	3322	6463	15
H(3C)	6374	2896	6071	15
H(2A)	6744	4543	4801	14
H(2B)	7869	4282	5245	14
H(2C)	7593	5589	4981	14

Table S6 Torsion angles [°] in compound **2**.

Co(1)-O(1)-C(1)-O(3)	177.31(18)
Co(1)-O(1)-C(1)-O(2)	-1.62(14)
Co(1)-O(2)-C(1)-O(3)	-177.32(17)
Co(1)-O(2)-C(1)-O(1)	1.63(15)

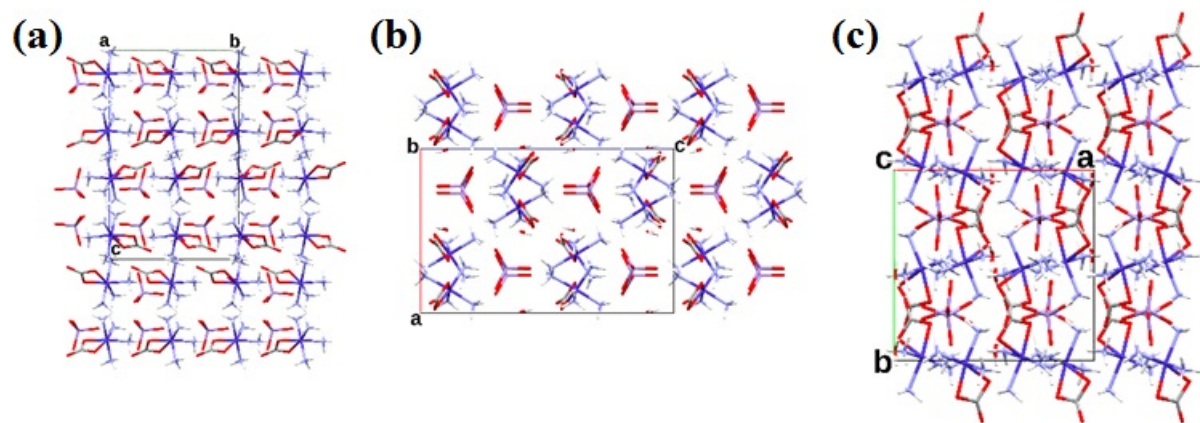


Figure S6 Crystal packing in compound **2**. View of the unit cell along the *a*, *b* and *c* axes.

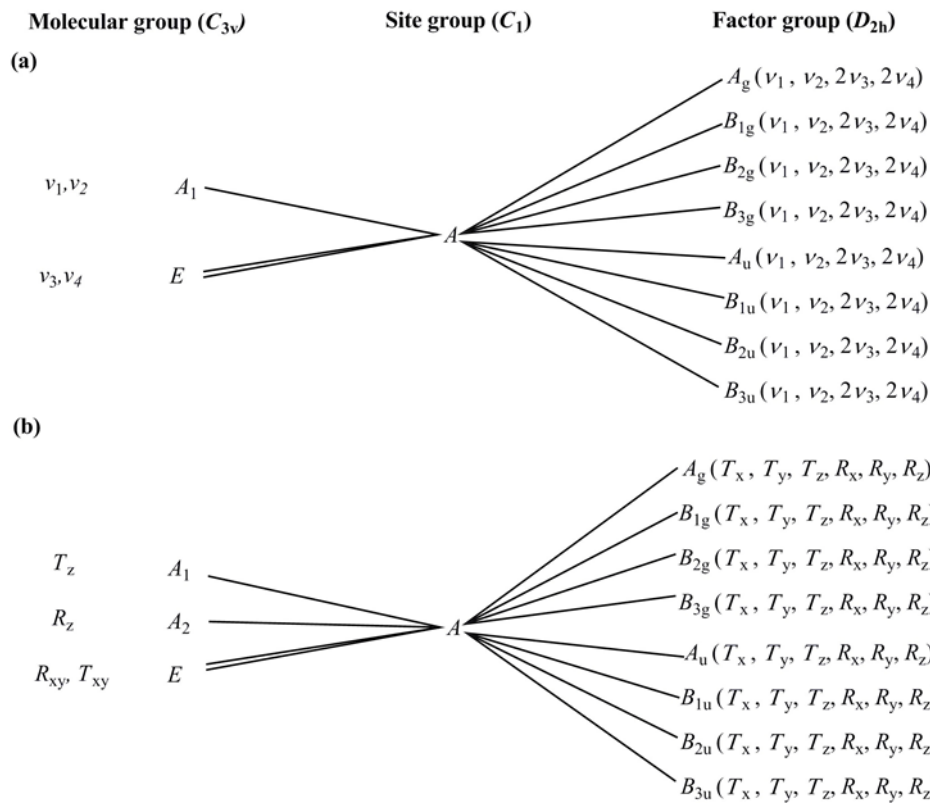


Figure S7 Correlation analysis diagram (a) internal and (b) external modes for ammonia ligands in compound 2.

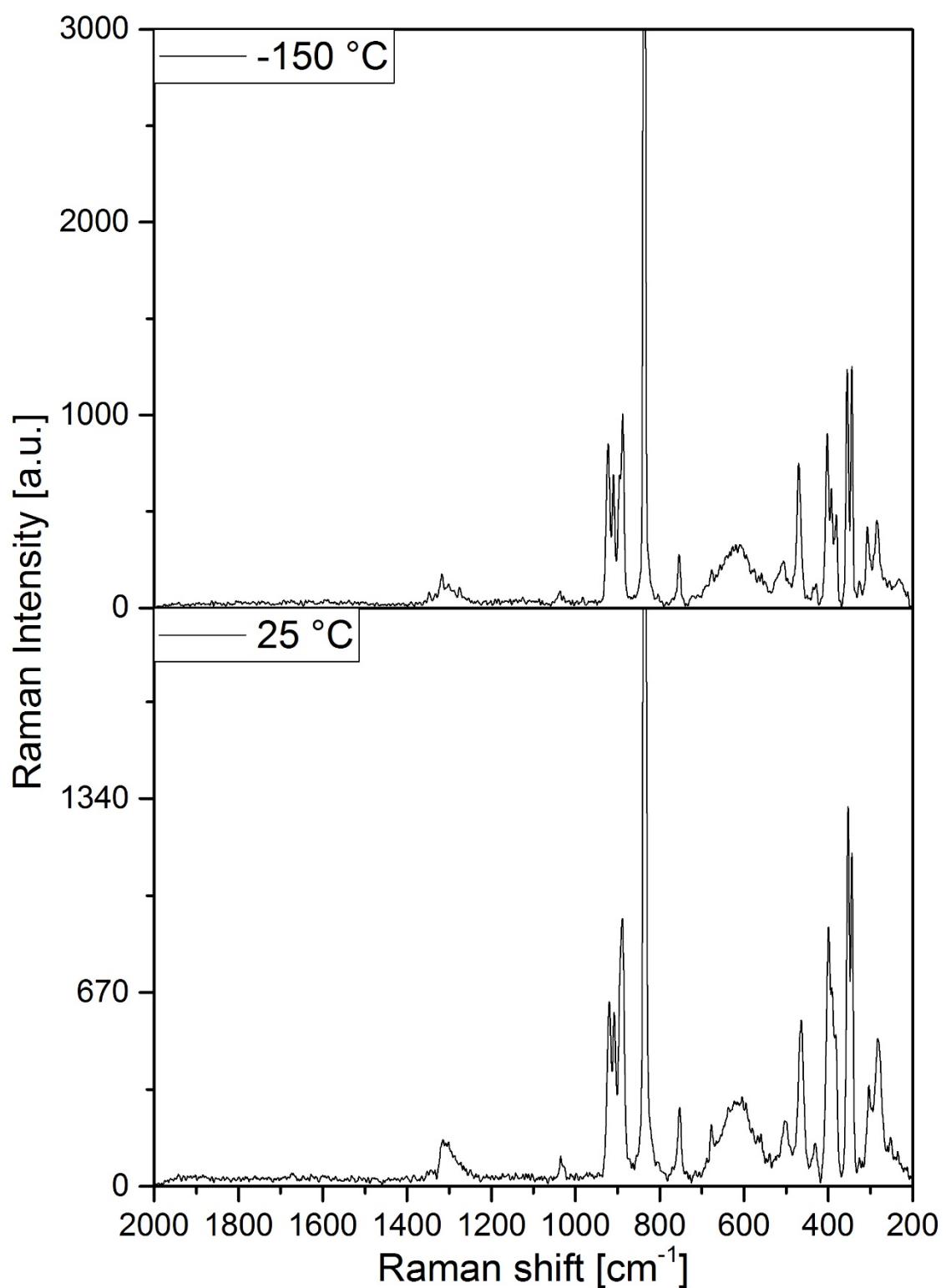


Figure S8 Raman spectra of compound **1** measured with 785 nm laser.

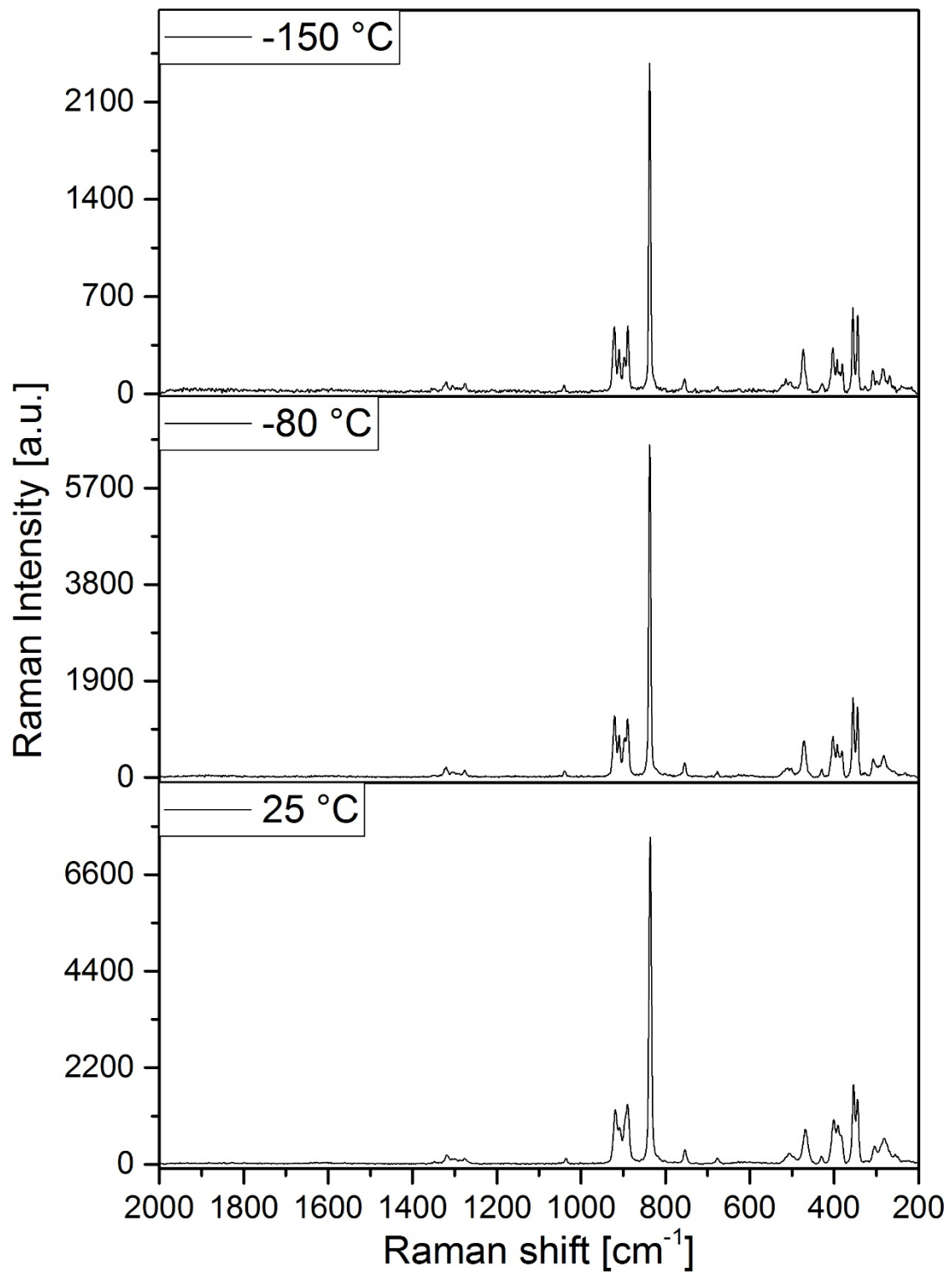


Figure S9 Raman spectra of compound **2** measured with 785 nm laser.

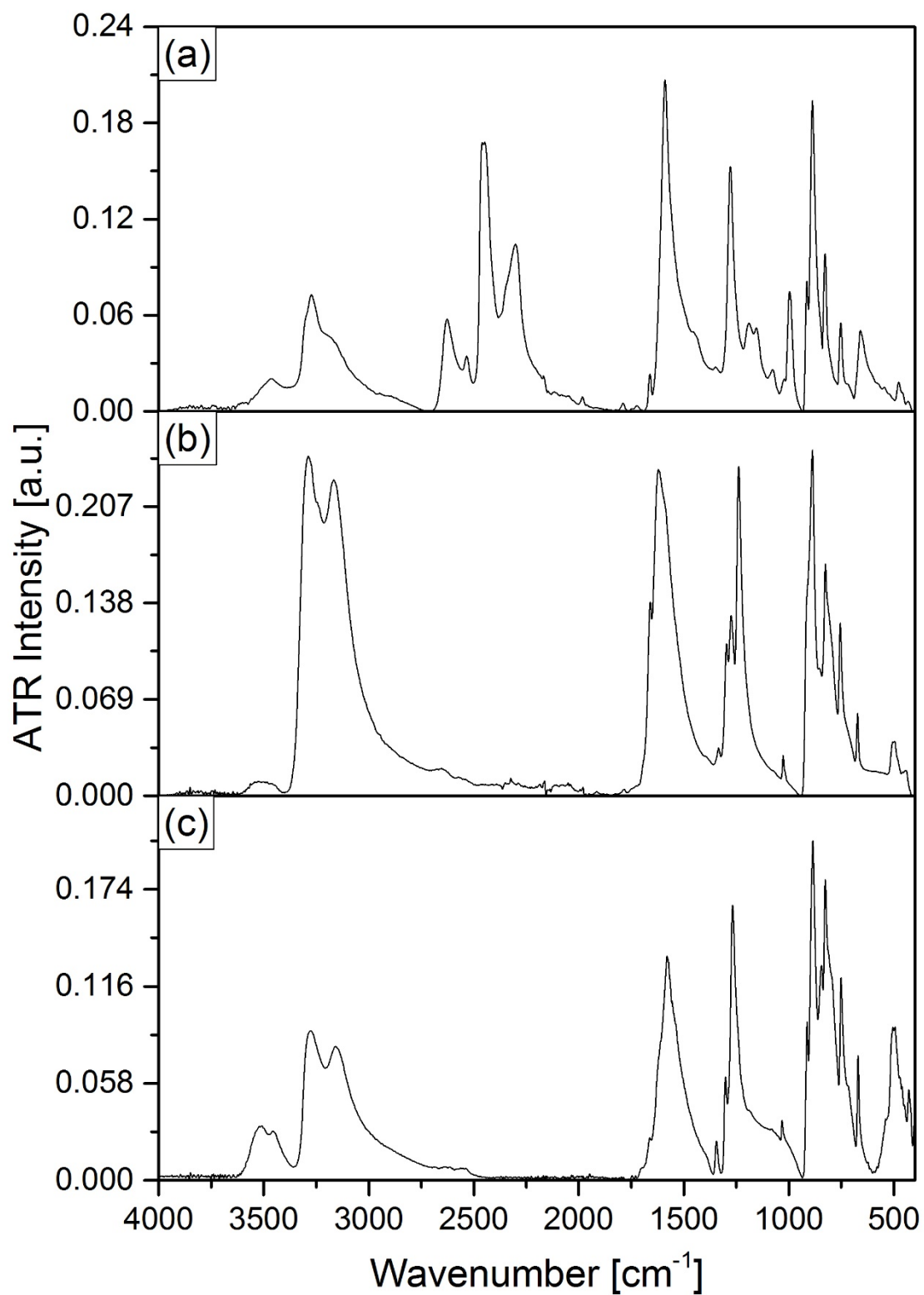


Figure S10 IR spectra of (a) compound 1, (b) compound 2, and (c) compound 2-D.

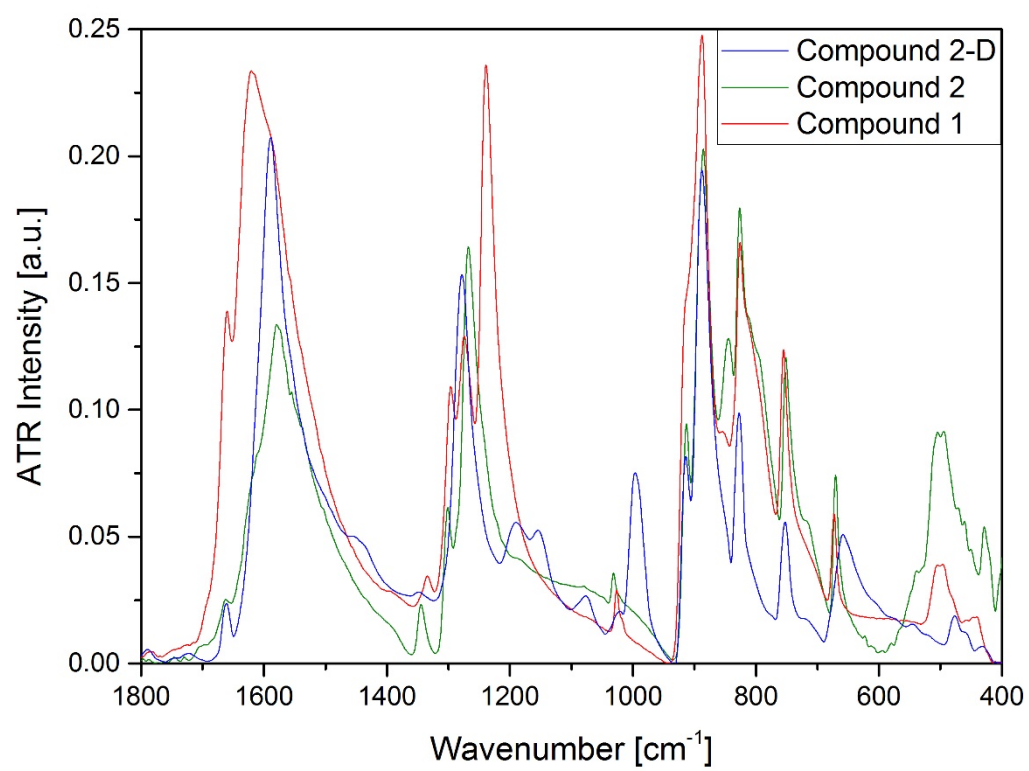


Figure S11 IR spectra of compound **1**, compound **2** and partially deuterated compound **2** (**2-D**) between 1800 and 400 cm⁻¹.

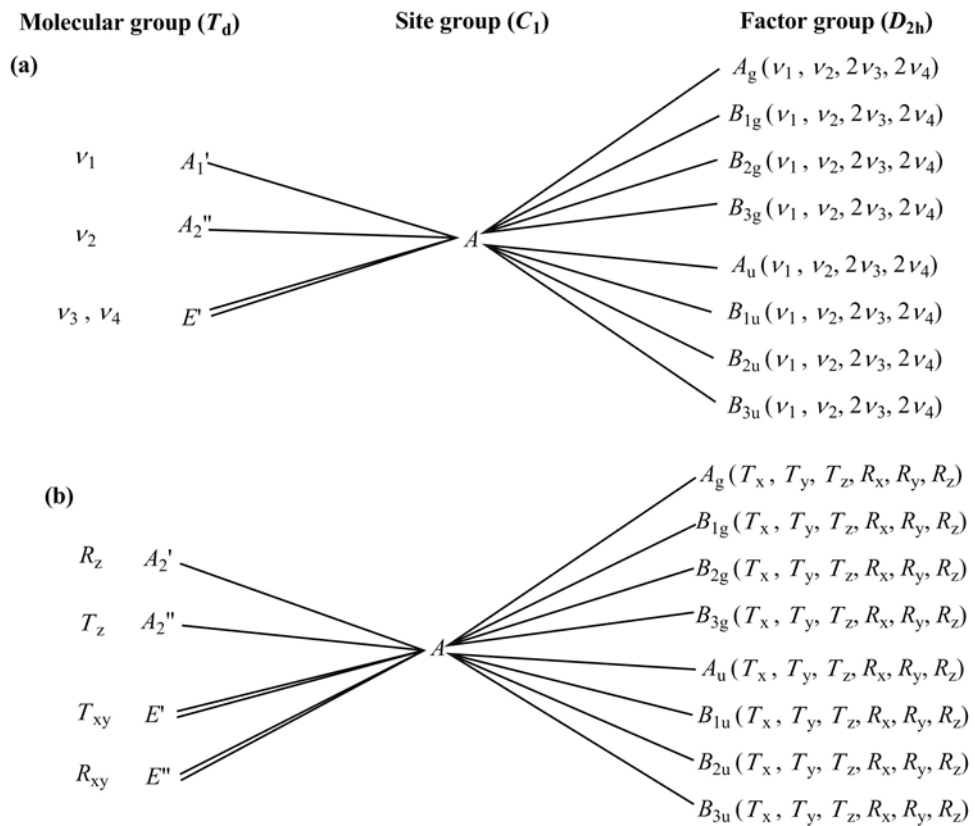


Figure S12 Correlation analysis diagram (a) internal and (b) external modes for carbonate ligand in compound 2.

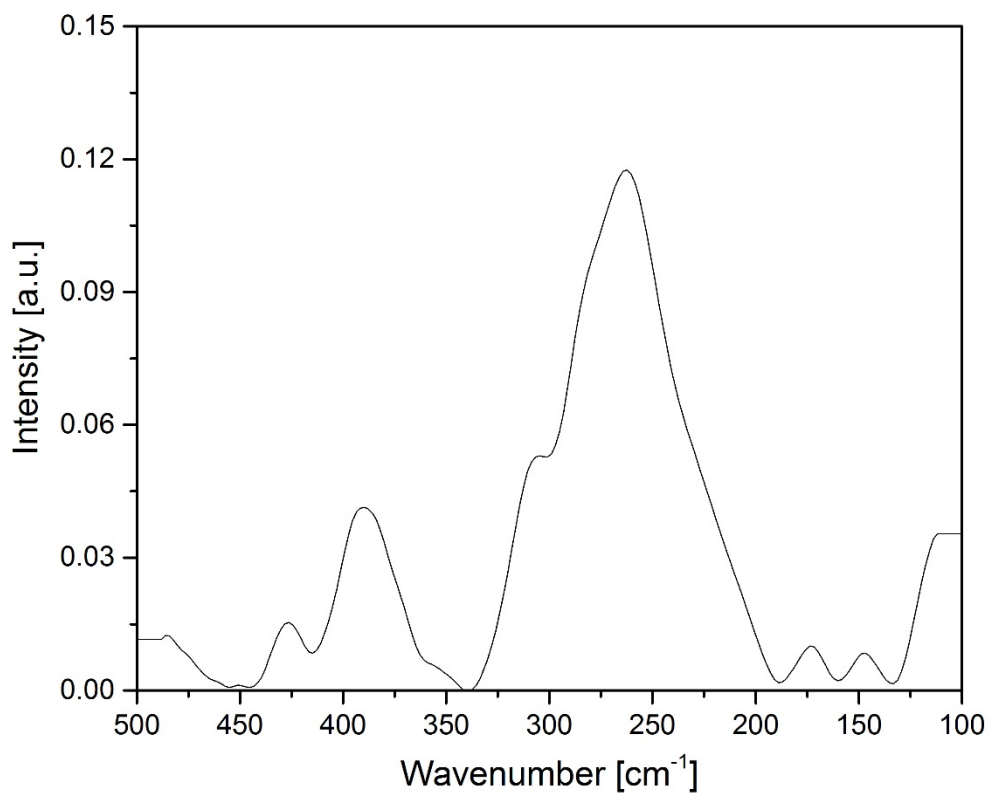


Figure S13 The far-IR spectra of compound 2.

Table S7 The internal vibrational modes of CoN_4O_2 core and their tentative assignments in the IR and Raman spectra of compounds **1** and **2**. (C_{2v} symmetry is assumed)

Species	Band	IR, 298 K		Raman (785 nm excitation)				Calculated, cm^{-1} [46]	Assignments		
		Compound 1	Compound 2	Compound 1		Compound 2					
				298 K	123 K	298 K	123 K				
A1	n_1	524	505	502	505	506	521, 514, 504	527	n_{CoN}		
	n_2	432	432	431	435,429	430	428	430	n_{CoN}		
	n_3	300sh	283	282	284	282	284	308	d		
	n_4	145	148	n.m.	n.m.	n.m.	n.m.	149	d		
	n_5	n.m.	n.m.	n.m.	n.m.	n.m.	n.m.	38	d		
	n_6	392*	390*	399*	403*	401*	403*	396	$n_{\text{as}}(\text{CoO})$		
A2	n_9	490sh	485sh	490	490	497	490	496	n_{CoN}		
	n_{10}	271	263	273sh	274sh	275sh	269	273	d		
	n_{11}	-	-	-	-	-	-	201	d		
B2	n_{12}	472sh	467sh	464	470	468	472	459	n_{CoN}		
	n_{13}	179	175	n.m.	n.m.	n.m.	n.m.	191	d		
	n_{14}	315sh	310	303	307	305	308	318	$n_s(\text{CoO})$		
	n_{15}	118	112	n.m.	n.m.	n.m.	n.m.	129	d		

*Overlapped band with $\delta_{\text{as}}(\text{Mn-O})$; > n.m.-Not measured (out of measurement range)

Table S8 Assignment of the permanganate vibrational modes in the IR and Raman spectra of compounds **1** and **2**.

Normal mode	IR, cm ⁻¹		Raman shift, cm ⁻¹			
	Compound 1	Compound 2	Compound 1		Compound 2	
			298 K	123 K	298 K	123 K
$\nu_s(\text{Mn-O})$	853	847	836	836	836	837
$\delta_s(\text{Mn-O})$	-	360sh	353,345	355,345	354,344	355, 345
$\nu_{as}(\text{Mn-O})$	914sh, 887	914,887	920, 908, 889	923, 910,896sh ,888	919, 909, 891	921, 910, 897, 889
$\delta_{as}(\text{Mn-O})$	392	392	399*, 391,383	403*, 393, 381	401*, 391, 383	403*, 393,381

*Overlapped bands

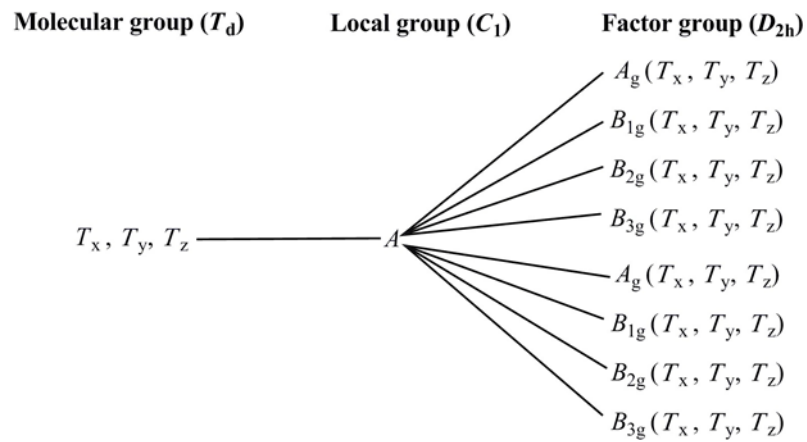


Figure S14 Correlation analysis diagram for central Co^{III} ion in compound **2**.

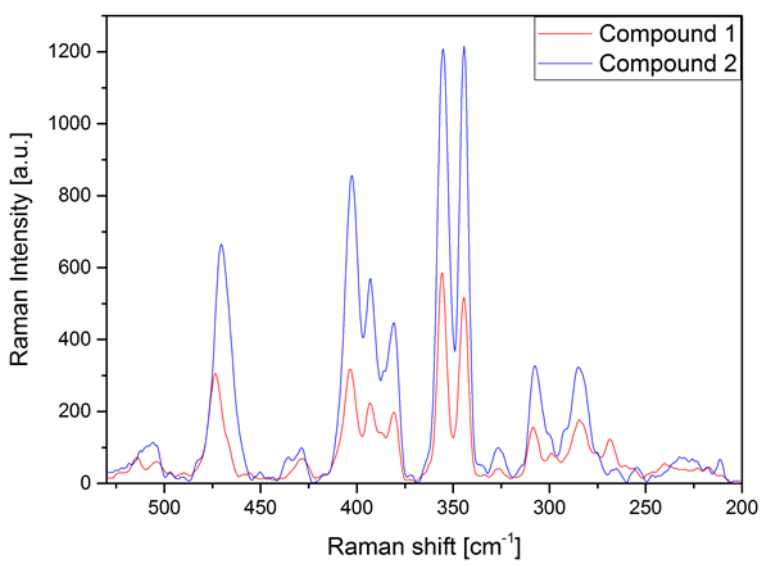


Figure S15 The Raman spectra of compounds **1** and **2** recorded at 123 K in the far-IR region.

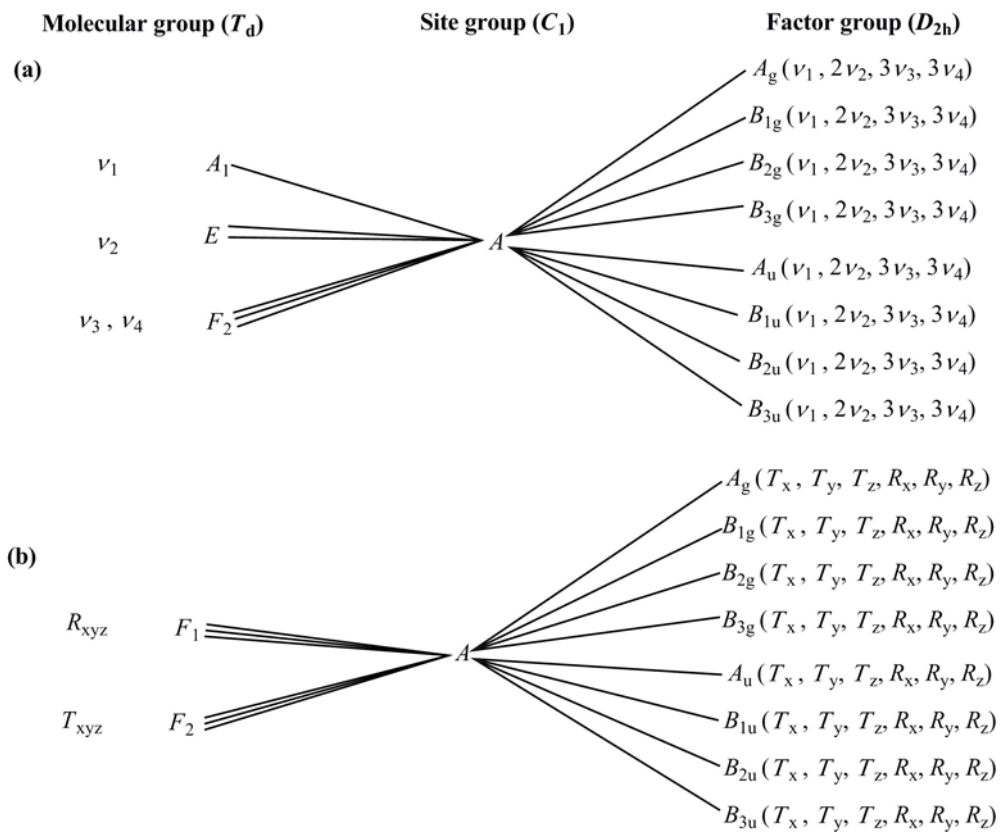


Figure S16 Correlation analysis diagram for the permanganate ion in compound 2.

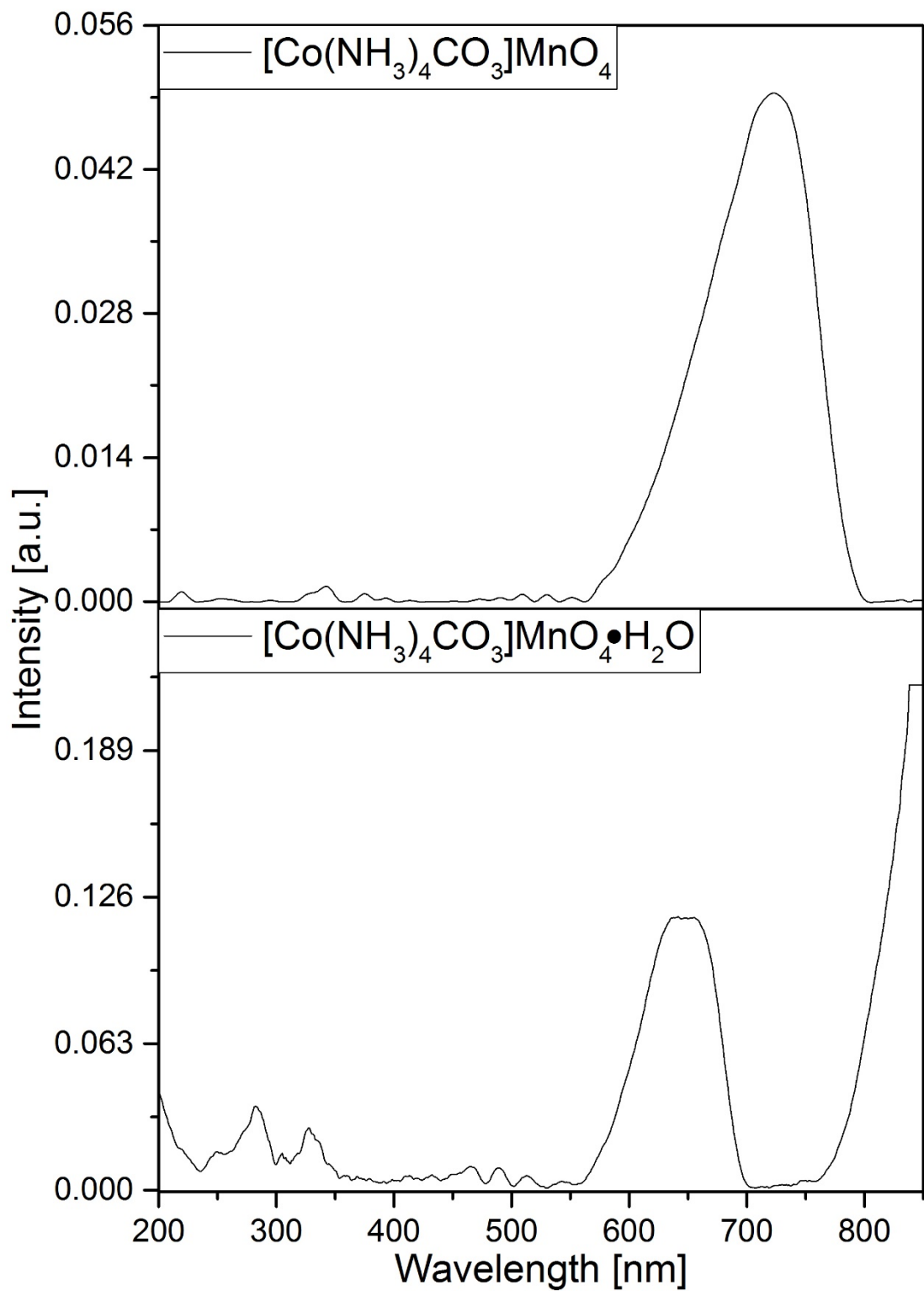


Figure S17 UV-VIS spectra of compounds 1 and 2.

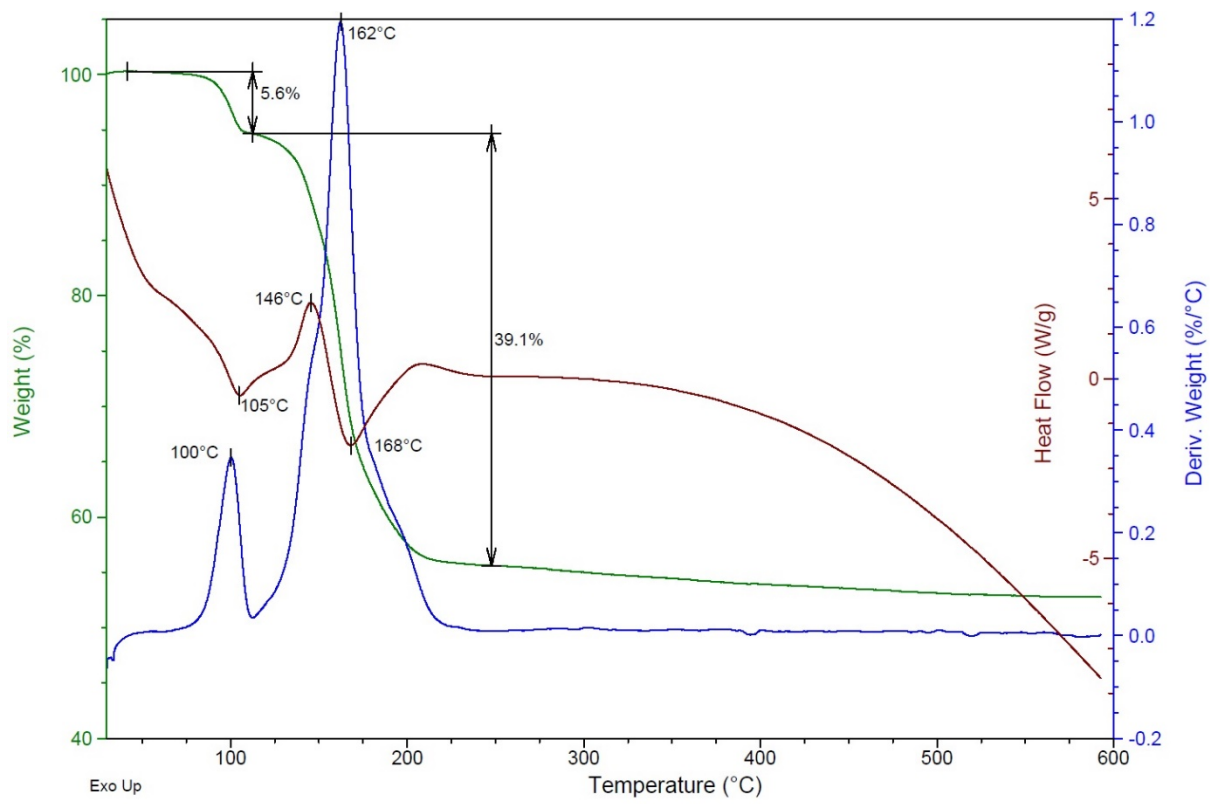


Figure S18 TG (green), DTG (blue), and DTA (curve of compound **2** in an inert atmosphere

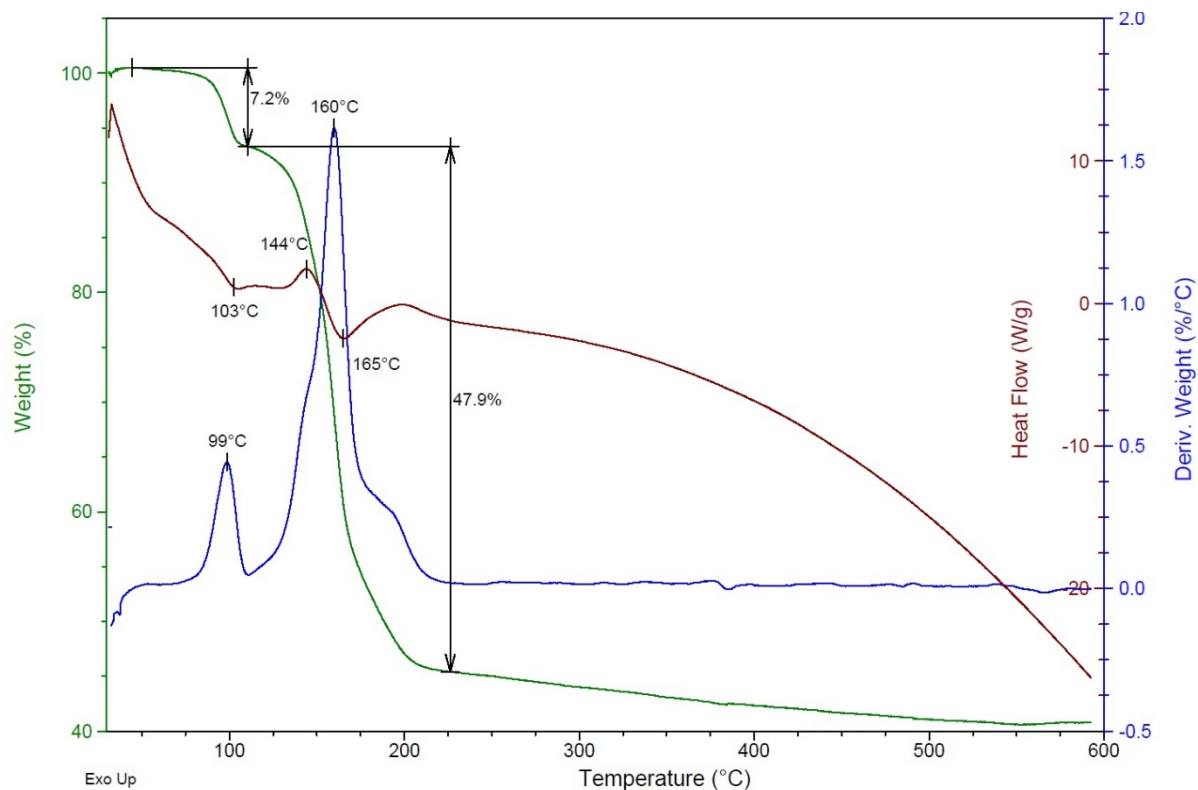


Figure S19 TG (green), DTG (blue), and DTA curve of compound **2** in air.

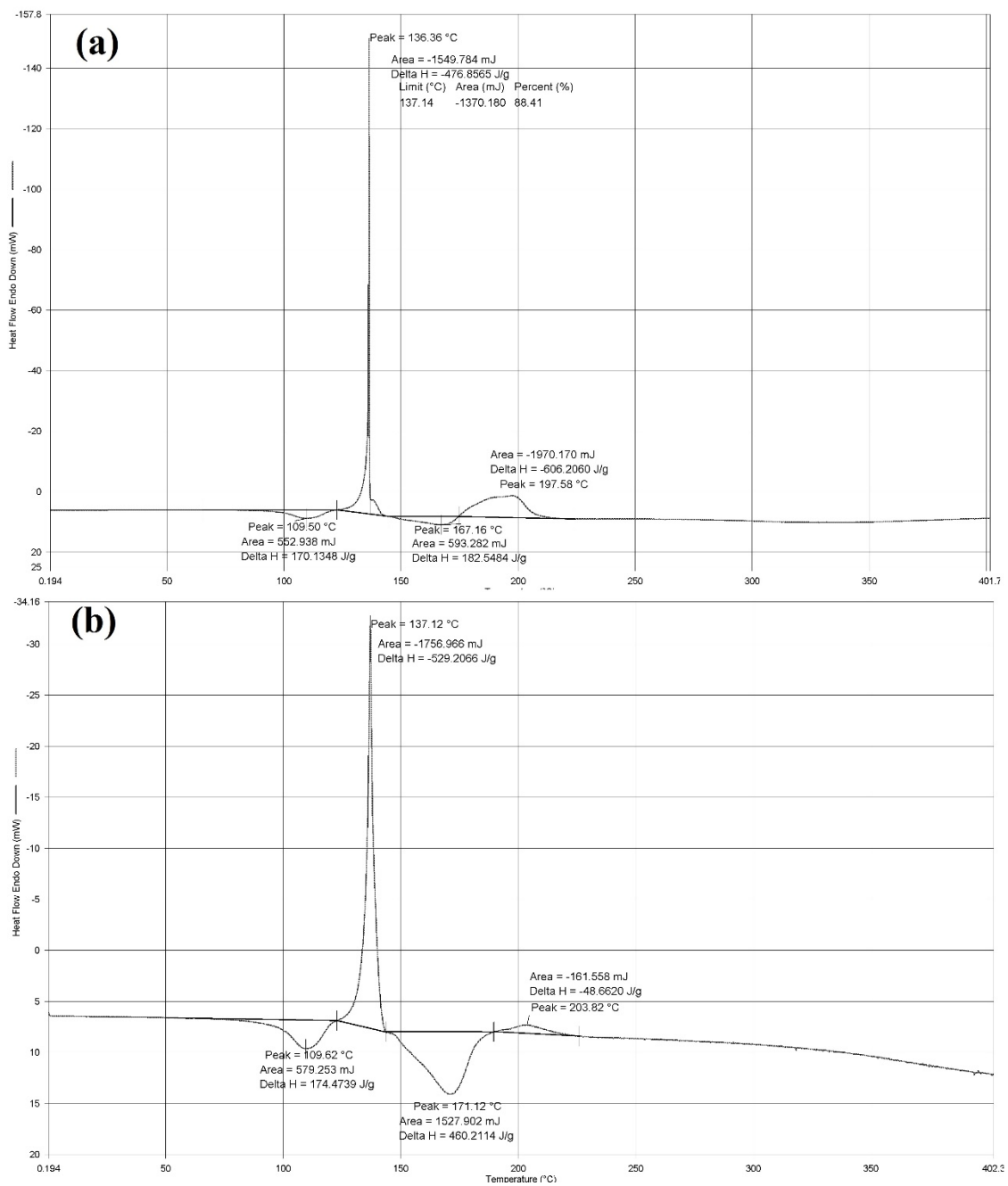


Figure S20 DSC of compound **2** under in an **(a)** O₂ and **(b)** N₂ atmosphere.

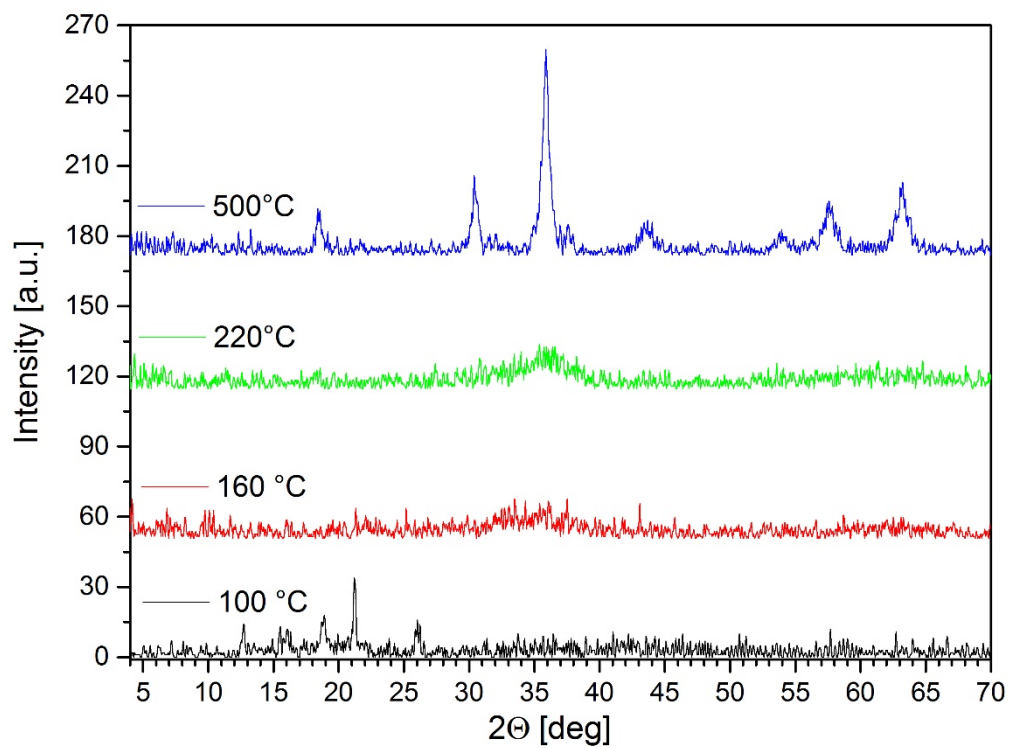


Figure S21 PXRD of the thermal decomposition products of compound **2** under an inert atmosphere (I-100 (compound 1), I-160, I-200 and I-500).

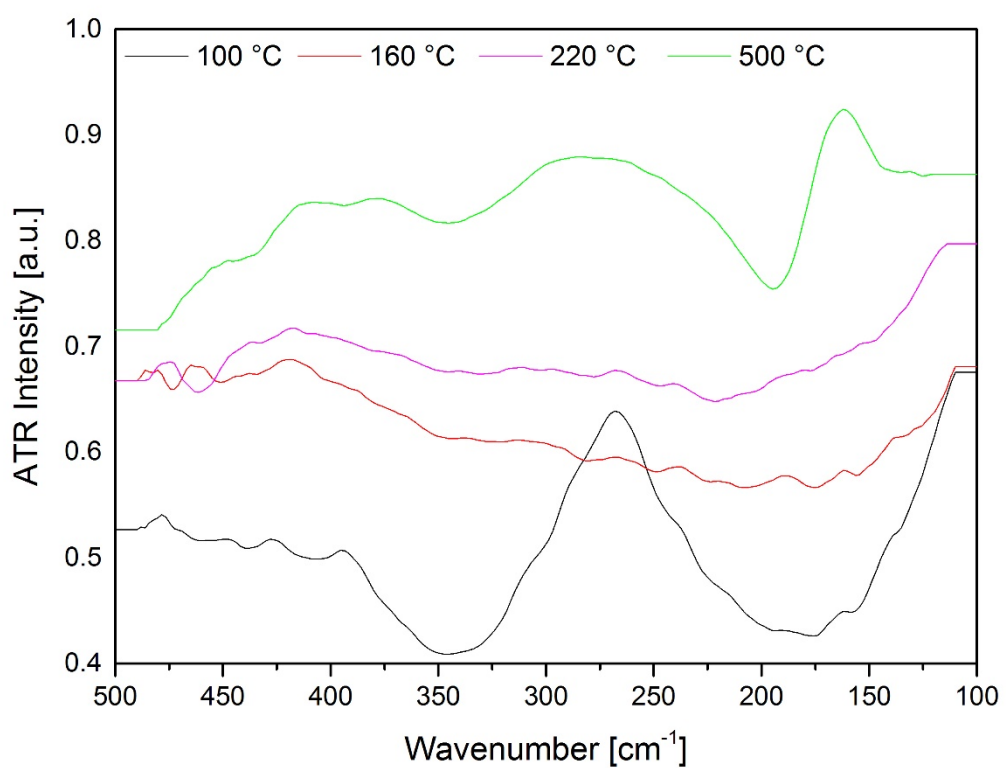


Figure S22 Far-IR spectra of the thermal decomposition products of compound **2** under an inert atmosphere.

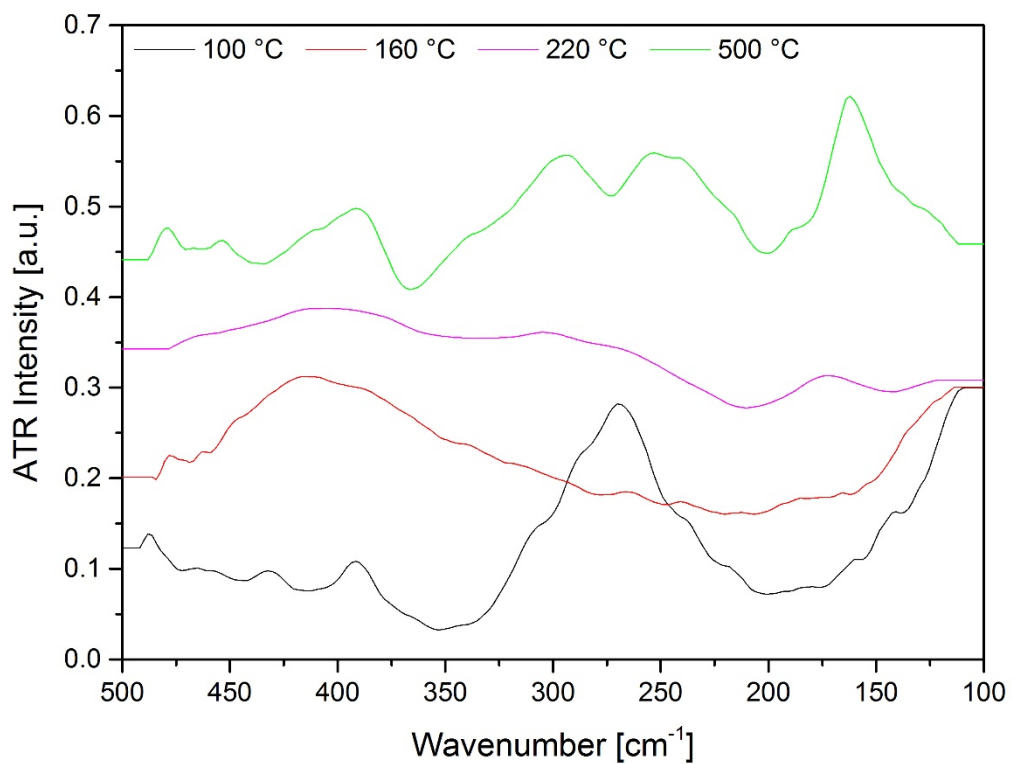


Figure S23 Far-IR spectra of the thermal decomposition products of compound **2** under an aerial atmosphere.

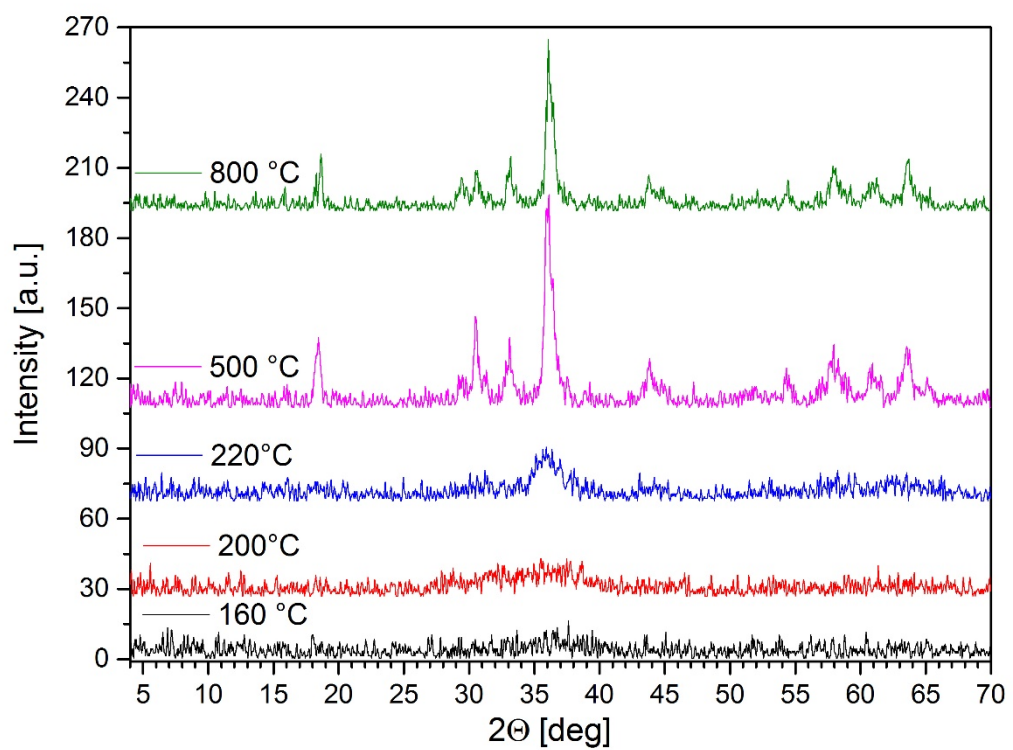


Figure S24 PXRD of the thermal decomposition products of compound **2** under an aerial atmosphere.

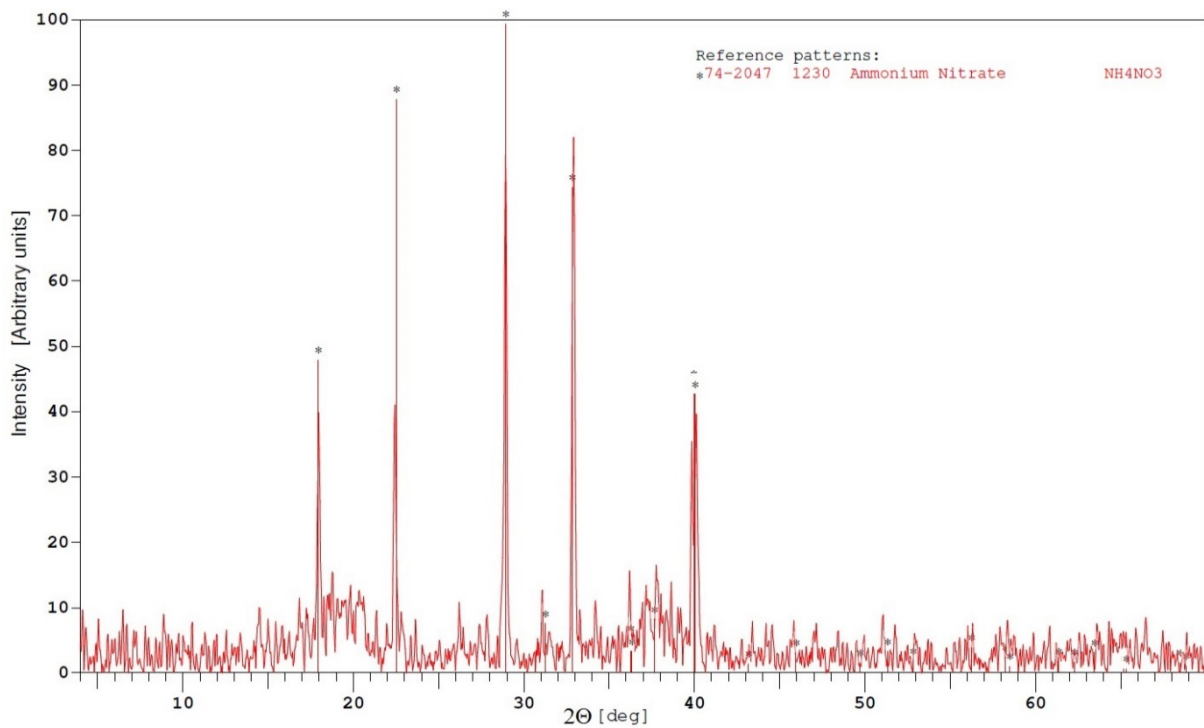


Figure S25 PXRD of water-soluble product of I-110 °C.

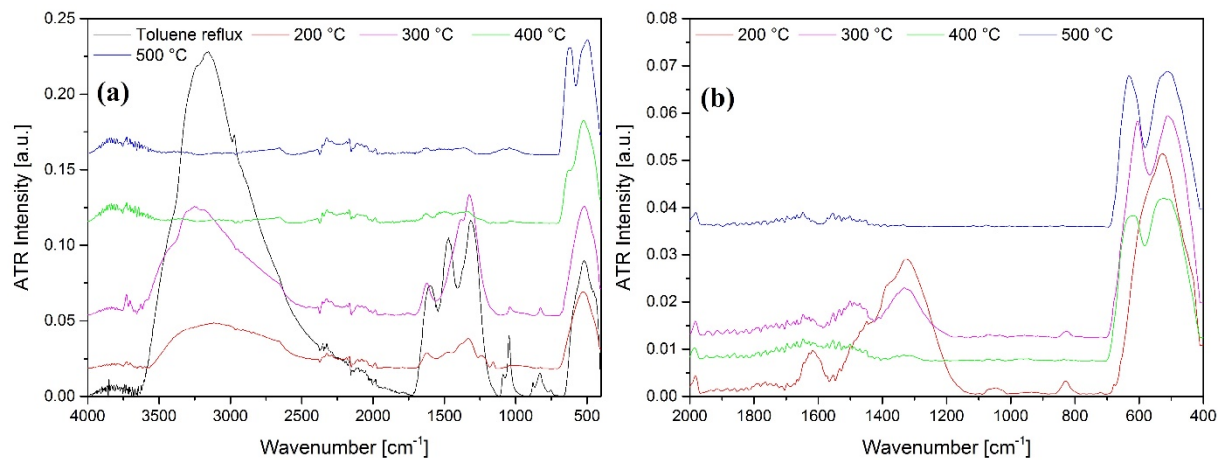


Figure S26 IR spectra of the thermal decomposition products of compound **2** under boiling toluene and after under air. Heat treatment **(a)** without and **(b)** with water soluble part (left back after decomposition in toluene).

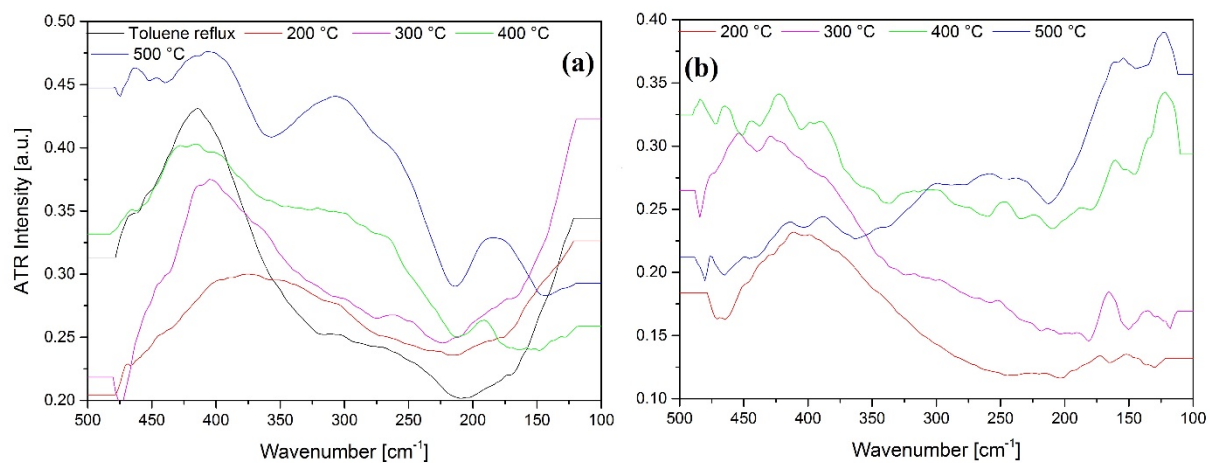


Figure S27 Far-range IR spectra of the thermal decomposition products of compound **2** under boiling toluene and after under air. Heat treatment **(a)** without and **(b)** with water soluble part (left back after decomposition in toluene).

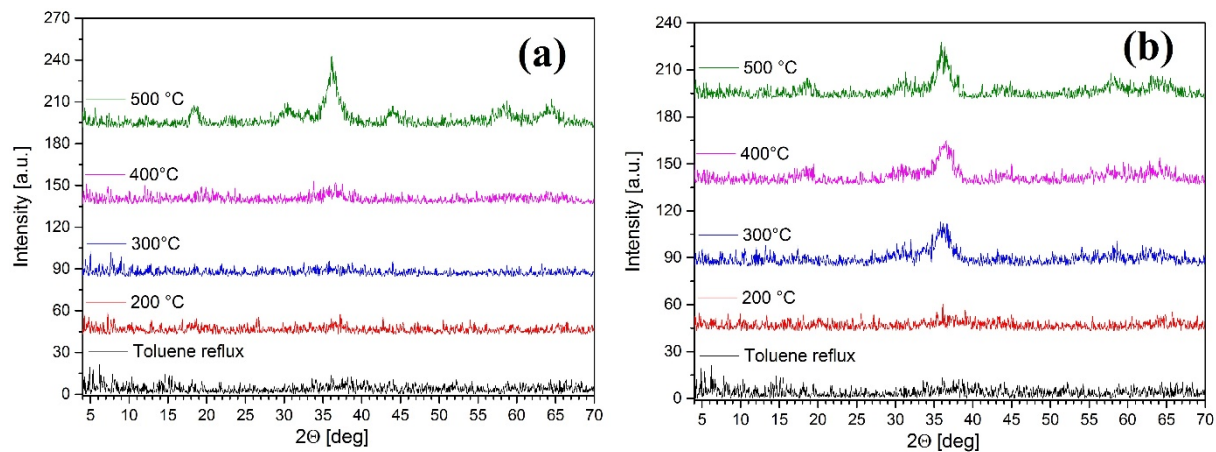


Figure S28 PXRD of the thermal decomposition products of compound 2 under boiling toluene and after under air. Heat treatment **(a)** without and **(b)** with water soluble part (left back after decomposition in toluene).